International Journal of Modern Research in Engineering & Management (IJMREM)
||Volume|| 2 ||Issue|| 7 ||Pages|| 09-16 || July 2019 || ISSN: 2581-4540

Annealing effecting on some properties of CTAB modified Tellurium dioxide thin films by hydrothermal Technique

[1,]Sozan A. Hassan , [2,]Sabri J. Mohammed
[1] *Department of Physics, College of Science, University of Kirkuk, Kirkuk, Iraq*
[2]*Department of Physics, College of Education, University of Tikrit, Tikrit, Iraq*

----------ABSTRACT----------
modified with hexadecyl trimethyl ammonium bromide (CTAB), the investigation of nanostructural and optical properties of TeO2 thin films was studied. The films are performed on glass substrates, the concentration of CTAB and hydrothermal treatment temperature played crucial roles and used as the parameters to control morphology by hydrothermal technique. At room temperature and annealing by tubular quartz furnace at temperature (473,673) K for 8 hours with air. XRD measurements showed that the structure for all samples is polycrystalline with a Tetragonal nanostructure. Surface morphology was studied using field emission scanning electron microscopy FESEM, Energy-dispersive X-ray spectroscopy, and atomic force microscopy AFM. After annealing, the roughness of the surface and the mean grain size were increased. Optical properties as a function to wavelength in the range (300-1100 nm) have been studied. Absorption spectra of Teo2 thin films showed that the absorption coefficient decreases with increasing annealing temperature. Direct energy gap for a Teo2 thin film was increased with increasing temperature for all samples due to crystal growth.

KEYWORDS: *Hydrothermal synthesis; Nanoparticles; Tellurium dioxide; CTAB*

Date of Submission: Date, 01 August 2019 *Date of Publication: 12 August 2019*

I. INTRODUCTION

Nanotechnology is a fast-growing discipline of the high-tech economy. Products of nanoparticles or nanomaterials (substances with particle sizes less than 100 nm) became a part of everyday life and the focus of many industries including cosmetics, clothing, foods and drug products , Although may cause adverse health effects on human, animal, and environment, the different properties of nanoparticles compared to their respective bulk materials such as a high surface area to volume ratio, new mechanical, chemical, electrical, optical, magnetic, electro-optical, and magneto-optical made them useful for many applications[1]. Consequently, careful environmental, human, and animal health safety assessment should be considered during the speedy commercialization of nanotechnology [2]. Recent research in nanomaterials is rapidly expanding into the assembly of well-ordered two- or three-dimensional (2D or3D) superstructures because, in many cases, the properties and applications of the materials are dependent on the spatial orientation and arrangement of the nanocrystals, more importantly, it allows the exploration of the collective properties of assemblies of particles. Many efforts have been focused on the fabrication of the self-assembled complex structures to achieve the goal of the integration of 1D nanostructures[3]. The physical and chemical properties of nanomaterials are dependent on their composition1 and morphology [4].

Low-dimensional semiconductor nanostructures such as nanowires (NWs), nanorods (NRs), nanobelts (NBs), and nanosheets (NSs) were widely studies due to their unique electrical and optical properties over traditional bulk materials, Due to considerable band-gaps of around 1.5–3.7 eV, one dimensional (1D) nanostructures draw a great deal of research attention for field-effect transistors (FET) and optoelectronic device applicati ons[5]. Among the 1D nanostructures, special emphasizes was given to semiconducting NWs due to its wide range applications in light-emitting diodes (LEDs), waveguides, lasers, sensors, photodetectors, solar cells, and FETs [6].Numerous semiconductor NWs were synthesized[7]. Among them, Tellurium oxide (TeO2) is a wideband (3.75 eV) p-type chalcogenide material available in both crystalline and amorphous phases . In the crystalline form, TeO2 exists in paratellurite(tetragonal) and tellurite (orthorhombic) phases, TeO2 has remarkable properties including high chemical stability, mechanical durability, high refractive index, good optical nonlinearity, electrical conductivity and piezoelectricity, which makes it suitable for various applications , Tellurium oxide thin films have been prepared by various techniques such as reactive[8] , sputtering including RF sputtering, thermal evaporation, sol-gel, hydrothermal method ,dip-coating and chemical vapor deposition [9]. the solution phase routes such as hydrothermal, reflux and solvothermal processes are more widely employed to prepare one-dimensional Te simplicity, high efficiency, low cost, and environmental friendliness.

Furthermore, it is well known that the trigonal tellurium and selenium nanowires or nanotubes could be directly nucleated and grown from their aqueous solutions without the use of any physical templates due to their crystal structures consisting of extended and helical chains [10]. Tellurium dioxide (TeO2) finds a wide range of technological applications such as deflectors, modulators, dosimeters, optical storage material, laser devices and gas sensors [11] . Because of its versatile physical and chemical properties. However, there are only a limited number of reports on the synthesis of TeO2 1D nanostructures and, in particular, very few on the TeO2 1D nanostructure sensors. the origin of the enhancement of the sensing properties of the p-type TeO2 nanorods by functionalization with CTAB.

II. EXPERIMENTAL SECTION

Preparation: Tellurium dioxide was grown on a glass substrate by using a hydrothermal method. The substrates were cleaned with an adequate amount of acetone and ethanol. After cleaning, the substrates were rinsed with deionized water and dried at room temperature. The hydrothermal synthesis was carried out for (2.5mmole) Potassium tellurite (K2TeO3) dissolved in 50 ml deionized water and then (2.5mmole) oxalic acid was added to the system to form a transport solution. The resulting solution was. Stirred for 15 minutes. Then, HCl was slowly added into the resulting solution to obtain a pH of 1. Then (0.25 mmole) CTAB was added into the solution. After stirring 30 min, the mixture was transferred into a 100 mL Teflon-lined stainless autoclave with filling about 60% of the whole volume by mixing distilled water. Glass substrate was dipped vertically in the autoclave, maintained at 160o C for 6h allowed to cool down at room temperature overnight. Teo2 thin films were washed with distilled water and ethanol for three times to neutralize the pH of the solution respectively and dried at 80∘ C for three hours. To observe the effect of CTAB, the product without the assistance of CTAB was synthesized maintaining the same condition.Finally, the thin films were annealed at deferent temperatures (473,673) k in the oven for eight hours for investigating the crystal structure, morphology, and optical properties.

Characterizations The Particles size and morphology were examined under vacuum by field emission scanning electron microscopy (FESEM). Fitted with Energy-dispersive X-ray spectroscopy (EDAX) [Model: FE-SEM. TESCAN MIRA3/RAITH LIS. France]. EDX analyses were used to confirm the compositions of the prepared nanomaterials. XRD measurements were performed using an Analytical X'Pert PRO diffractometer and Cu Ka radiation (λ= 0.15418 nm); the samples were prepared on glass substrates. UV-Vis absorption spectra of the colloids were recorded using a double-beam UV-Vis spectrophotometer Shimadzu.

III. RESULTS AND DISCUSSION

FESEM and AFM Compositional analysis: FESEM images for TeO2 thin films prepared with CTAB by hydrothermal method at (160 oC) deposited on the glass substrates, then annealed at different temperatures with magnification powers (x3k), (x30 k), (x50 k) were shown in figure (1). The samples appear in multi-surface structures of various shapes and sizes, including longitudinal and other eight -surface forms with big diameter and nanostructure miraged with each other. These forms weakly contact between them, in the samples prepared at room temperature. After annealing, the surfaces become smoother and the nanostructure miraged to each other more and more as the increase of annealing to form a composition in the form of a network with a high surface area in addition to good contact between grains. This structure suggests an excellent sample to be used in gas sensor applications due to small nanoparticles with a large surface area of gas interaction with them and related to a neck connection between them. Also, the high sample porosity allowing gas penetration within the sample to interact with a large area.

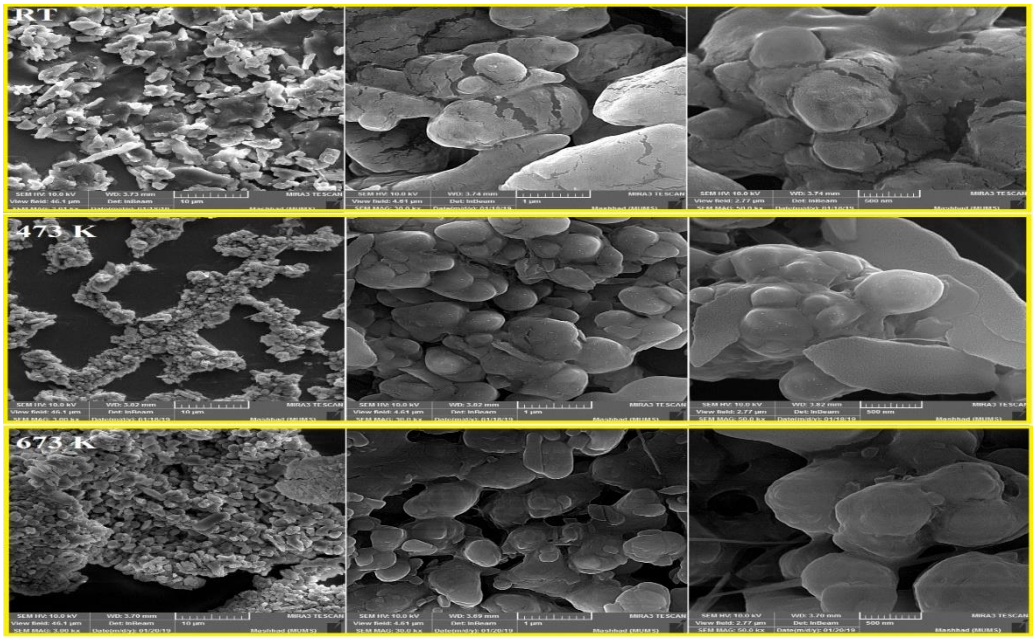

Figure (1): FESEM images at different magnification powers for TeO2 thin films prepared with CTAB annealed at different temperatures (RT, 473, 673) K

Figure (2) shows the results of the TeO2 thin films prepared with CTAB at different temperatures. Two peaks are noticed corresponding to tellurium (Te), located at about 4 and 4.5 keV corresponding to Kα and Kβ transitions, respectively. Whereas oxygen peak (O) appeared at about 0.5 keV represented with different intensities depending on their ratio in the sample. In addition to peaks corresponding to the glass substrate specially for (Br) peaks, silicon, sodium, and magnesium. The ratio of weight percentage and atomic percentage were calculated by the program attached to the examination device, using peak intensities for Kα transition. It is observed that the oxygen ratio increased with respect to tellurium with CTAB.

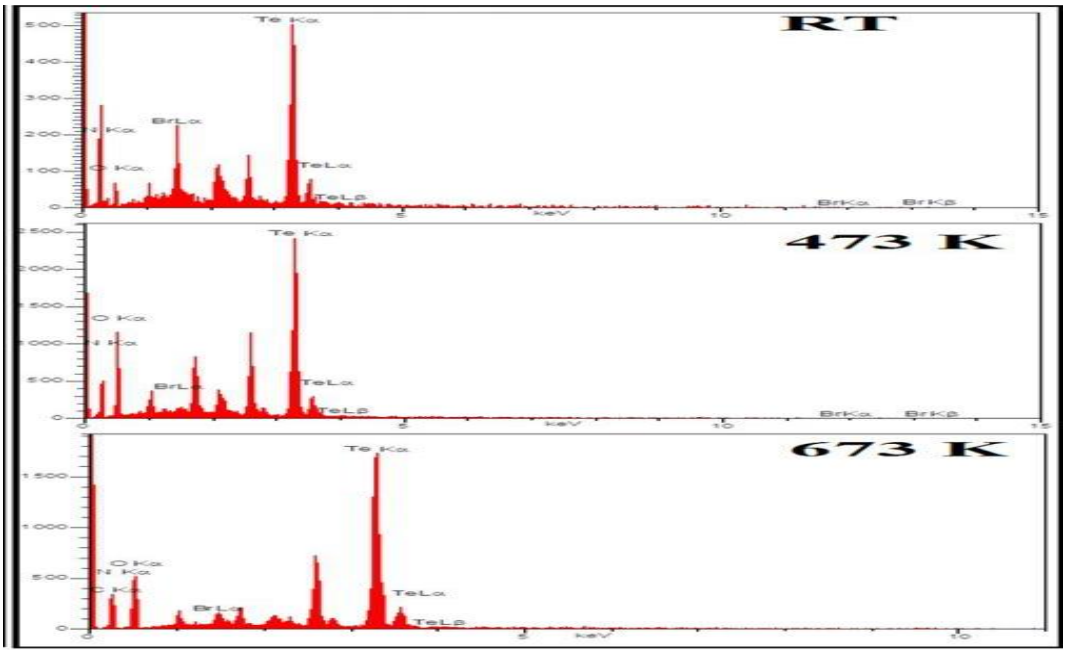

Figure (2): EDX analysis for TeO2 thin films samples annealed at different temperatures prepared with CTAB.
The atomic force microscope (AFM) gives information about surface topography of the examined sample in the nano range. Figure (3) shows the atomic force microscopy images and the granularity distribution histogram for TeO2 thin films prepared with CTAB by hydrothermal process and deposited on a glass substrate and annealed at

different temperatures. This figure illustrates nanostructures, Uniformly distributed nanostructures with a narrow distributed histogram for RT sample. The average diameter increased after annealing at 473 K and be with wide particles size distribution. While annealing at 673 K cause to decrease particle diameters.

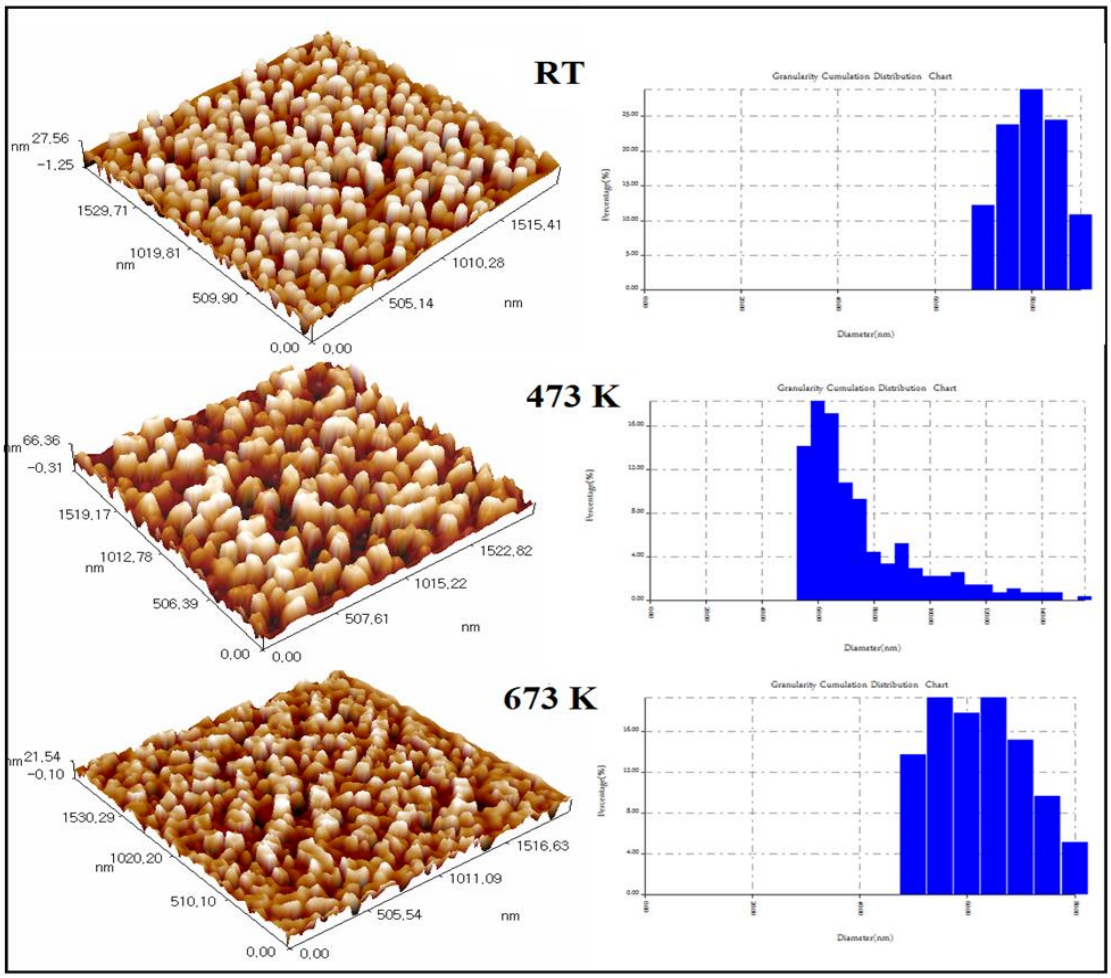

Figure (3): 3D AFM images and their granularity accumulation distribution for TeO_2 thin films prepared with CTBA annealed at different temperatures

The AFM parameters for TeO_2 thin films samples prepared with CTAB are shown in Table (1). The maximum roughness appeared at 473 annealing temperature. The sample prepared with CTAB appeared with roughness

Table 1: AFM parameters (Average Diameter, RMS roughness, and Roughness average) for TeO_2 thin films prepared with CTAB, annealed at different temperatures

samples	Temp K	Average Diameter (nm)	RMS roughness (nm)	Roughness Ave. (nm)
TeO_2 with CTAB	RT	72.94	6.16	7.09
	473	77.41	15.5	18.1
	673	60.19	4.21	3.06

Structural properties: Figure (4) shows the X-ray diffraction patterns for as prepared TeO2 thin films with CTAB on glass substrates and annealed samples at 473 and 673 K., polycrystalline structure for all samples with the same phases appeared. Annealing cause to enhance samples crystallinity. The peaks appeared with more broadening than samples prepared without CTAB, especially for (111) direction, indicate decreasing its crystalline size. Table (2) illustrates the structural parameters for TeO2 thin films samples prepared with CTAB

Table (2): XRD parameters for TeO2 thin films prepared with CTAB annealed at different temperatures

Ta (K)	2θ (Deg.)	FWHM (Deg.)	d_{hkl} Exp.(Å)	C.S (nm)	d_{hkl} Std.(Å)	Phase	hkl	card No.
RT	23.1398	0.4741	3.8407	17.1	3.8573	Hex. Te	(100)	96-900-9089
	26.1877	0.4742	3.4002	17.2	3.3976	Tet. TeO_2	(110)	96-101-1099
	28.4906	0.8128	3.1304	10.1	3.1024	Tet. TeO_2	(111)	96-101-1099
	29.4727	0.2710	3.0282	30.3	2.9827	Tet. TeO_2	(012)	96-101-1099
	38.2100	0.3386	2.3535	24.8	2.3493	Hex. Te	(012)	96-900-9089
	40.6144	0.4064	2.2195	20.8	2.2270	Hex. Te	(110)	96-900-9089
473	21.5143	0.3386	4.1271	23.9	4.0627	Tet. TeO_2	(101)	96-101-1099
	22.9705	0.4064	3.8686	19.9	3.8573	Hex. Te	(100)	96-900-9089
	27.6778	0.2709	3.2204	30.2	3.2324	Hex. Te	(011)	96-900-9089
	28.4228	0.5758	3.1377	14.2	3.1024	Tet. TeO_2	(111)	96-101-1099
	30.0484	0.5418	2.9715	15.2	2.9827	Tet. TeO_2	(012)	96-101-1099
	38.3116	0.3387	2.3475	24.8	2.3493	Hex. Te	(012)	96-900-9089
	40.5128	0.4064	2.2249	20.8	2.2270	Hex. Te	(110)	96-900-9089
673	21.8868	0.4742	4.0576	17.1	4.0627	Tet. TeO_2	(101)	96-101-1099
	23.2075	0.4741	3.8296	17.1	3.8573	Hex. Te	(100)	96-900-9089
	26.2893	0.4403	3.3873	18.5	3.3976	Tet. TeO_2	(110)	96-101-1099
	27.7455	0.3387	3.2127	24.2	3.2324	Hex. Te	(011)	96-900-9089
	28.4228	0.4402	3.1377	18.6	3.1024	Tet. TeO_2	(111)	96-101-1099
	29.9806	0.5400	2.9781	15.2	2.9827	Tet. TeO_2	(012)	96-101-1099
	37.5327	0.4064	2.3944	20.6	2.4025	Tet. TeO_2	(200)	96-101-1099
	38.2100	0.3387	2.3535	24.8	2.3493	Hex. Te	(012)	96-900-9089
	39.3953	0.3387	2.2854	24.9	2.2910	Tet. TeO_2	(201)	96-101-1099
	40.4112	0.3725	2.2302	22.7	2.2270	Hex. Te	(110)	96-900-9089
	48.6744	0.3726	1.8692	23.4	1.8710	Tet. TeO_2	(212)	96-101-1099
	50.0629	0.4742	1.8205	18.5	1.8339	Hex. Te	(021)	96-900-9089
	51.0111	0.5080	1.7889	17.3	1.7800	Hex. Te	(112)	96-900-9089
	58.3599	0.5419	1.5799	16.8	1.5673	Tet. TeO_2	(301)	96-101-1099
	66.1829	0.5080	1.4109	18.7	1.4157	Hex. Te	(121)	96-900-9089

The (111) direction has a crystalline size of 10.1 increase to 14.2 nm at 473 K and then to 18.6 nm at 673 K annealing temperature. Annealing remove the crystalline boundaries and merge the adjacent crystals.

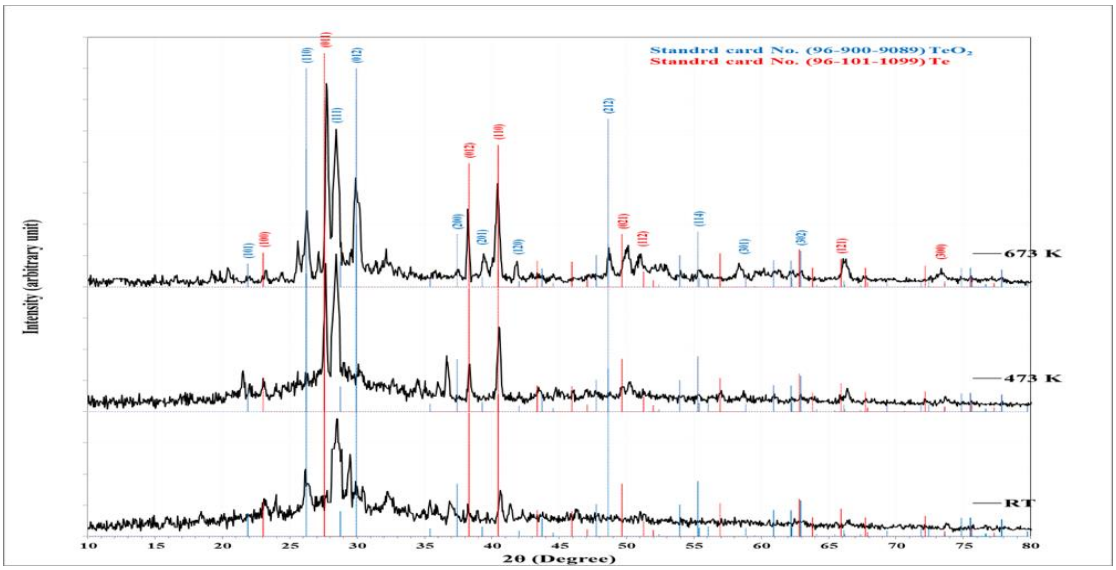

Fig. 4: XRD patterns for TeO2 thin films prepared with CTAB annealed at different temperatures

Optical properties the optical properties for TeO2 with CTAB deposited on glass substrates by hydrothermal method at (160 oC) and annealed at 473 and 673K were studied using UV-Visible transmission in the wavelength range 300–1100 nm.

Fig. (5) Illustrates the transmittance spectra for as-deposited TeO2 thin film samples prepared with CTAB and annealed at 473 and 673 K annealing temperature. The sharp fall in the transmittance at 350 nm wavelength is due to the strong absorbance of the films in this region.

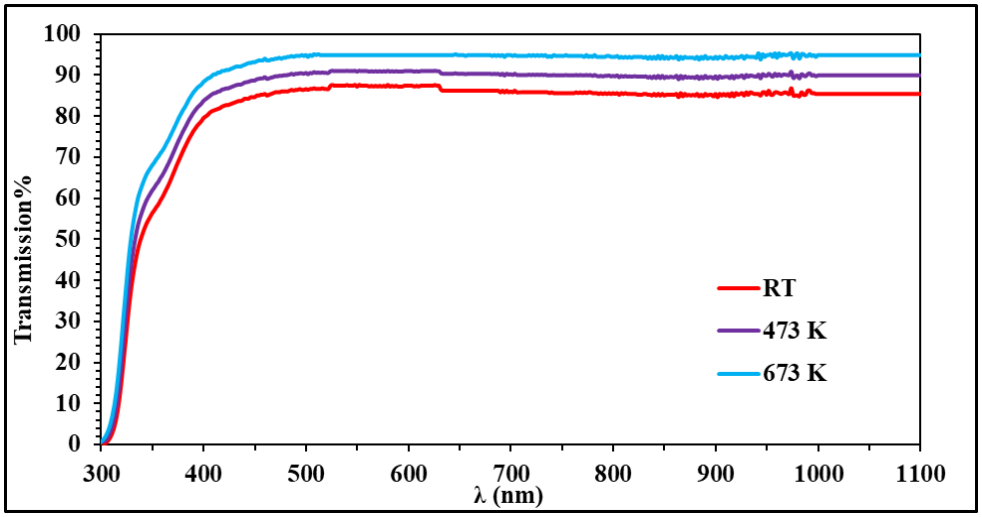

Figure (5): Transmission curves for TeO_2 thin films prepared with CTAB annealed at different temperatures

The fundamental absorption edge is one of the essential features of the absorption spectra, which provides the most valuable optical information available for material identification. The nature of the optical transition involved in the blends can be determined based on the dependence of the absorption coefficient (α) on photon energy ($h\nu$). Figure (6) shows the optical absorption coefficient α as a function of wavelength (λ) for TeO_2.thin films prepared with CTAB and annealed at different temperatures. We can see from this Figure that the values of α become higher ($\alpha > 10^4$) cm^{-1}, this supports to expect a direct electronic transition occurs in these regions. Also, we found that the α of the TeO_2 with CTAB films on glass substrate has a stable absorption coefficient at the short wavelength region (high energies). On the other hand, it is found that the value of α decreases with increasing of annealing temperature due to increase energy gap with wavelength.

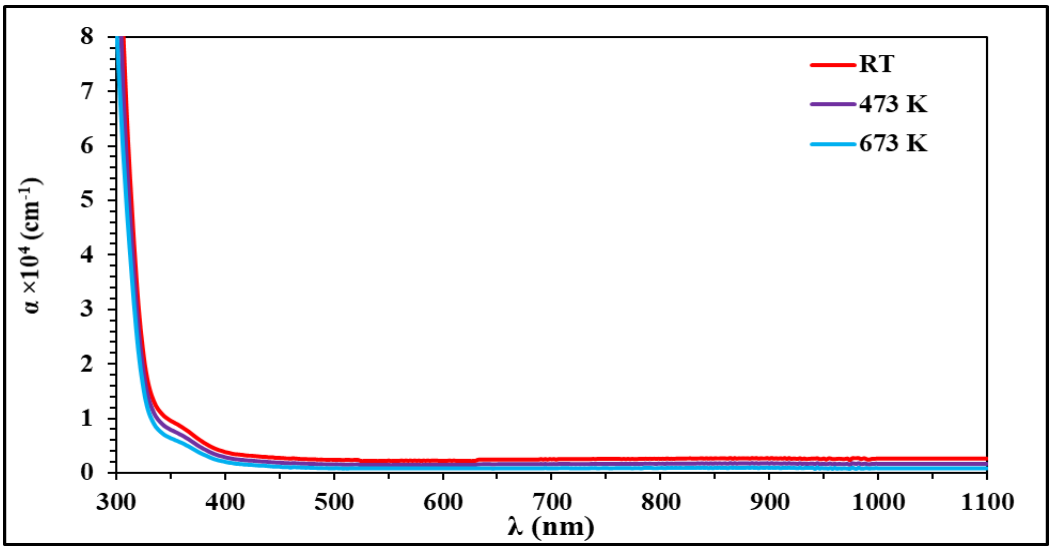

Fig. (6): Absorption for TeO_2 thin films prepared with CTAB annealed at different temperatures

The absorption coefficient (α) was calculated from the absorbance (A) using Lambert Beer's law[12],[13].

$$I = I_0 \exp(-\alpha d)$$

α= 2.303/d log(I/I_0) = 2.303A/d (2)

Where I_o and I are the intensities of the incident and transmitted radiation, respectively, d is the thickness of the sample in cm. The absorption coefficient (α) of bandgap material is given by:

$\alpha h\upsilon=\beta(h\upsilon-Eg)^{\gamma}$ (3)

where Eg is the energy bandgap, constant β is a constant related to the properties of the valance band and conduction band, also is a useful diagnostic of the material. $h\upsilon$ is the energy of photons, and γ is an index used to be assumed the values 1/2, 3/2, 2 or 3 depending on the nature of the electronic transition, corresponding to allowed direct, forbidden direct, allowed indirect and forbidden indirect transitions, respectively. According to Tauc's extrapolation, the band gap of a material can be obtained from the extrapolation of the straight-line portion of the $(\alpha h\upsilon)^{1/n}$ against $h\upsilon$ to α=0. The direct bandgap values were obtained by plotting $(\alpha h\upsilon)^2$ versus $h\upsilon$ curves, as Fig. (6) Illustrates the transmittance spectra for as-deposited TeO_2 thin film samples prepared with CTAB and annealed at 473 and 673 K annealing temperature. The sharp fall in the transmittance at 350 nm wavelength is due to the strong absorbance of the films in this region. The values of the optical energy gap Eg for nanoparticles TeO_2 thin films prepared with CTAB and annealed at different temperatures. A plot of relation $(\alpha h\upsilon)^2$ versus photon energy ($h\upsilon$) and the choice of the desired linear section. From Figure (7) we can see that the energy gap was increased from (3.85-3.9) eV, as a result of the increasing of the annealing temperature, this is due to the growth of grain size and the reduction of the number of grain boundaries. Increase Eg as a result of reducing the amount of absorption; this may lead to improve the crystal structures, which leads to the reduction of defects (tail state) in the forbidden gap and this leads to an increase in the Eg.

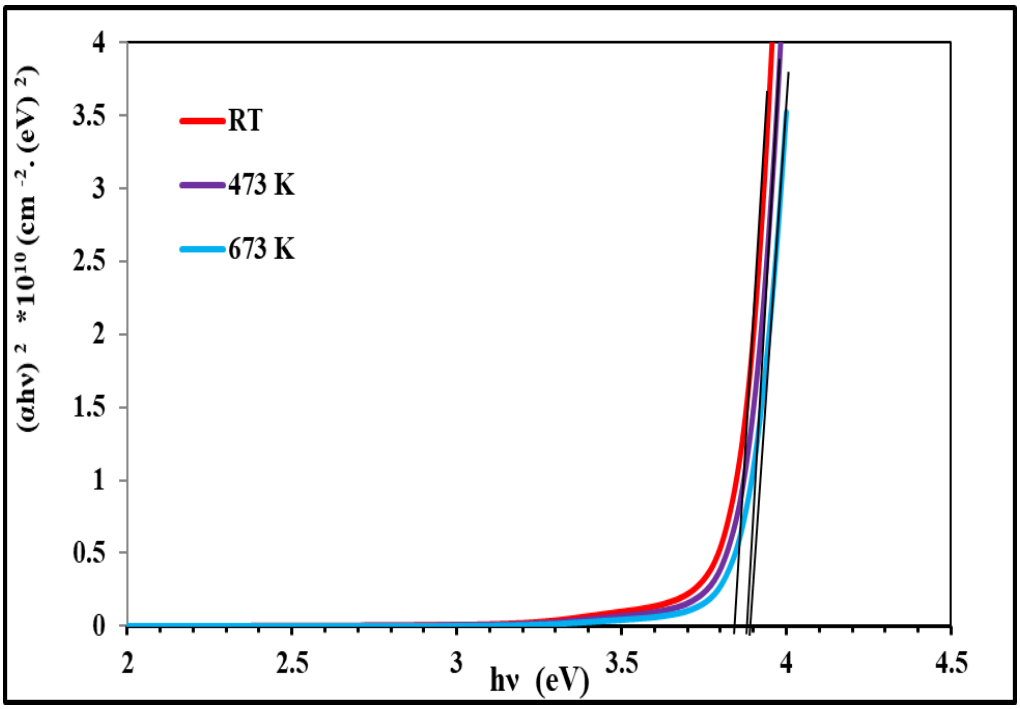

Fig. (7): Tauc relation for TeO_2 thin films prepared with CTAB annealed at different temperatures

IV. CONCLUSION

In summary, a nano structured of CTAB modified Tellurium dioxide thin films was synthesized by a novel hydrothermal method, Post-annealing process helps to improve the crystalline quality thin films. All the films show polycrystalline with Tetragonal nanostructure. Were characterized by FESEM, EDX, and AFM . indicate that the Average Diameter, roughness Average and RMS of the nanoparticles thin film increases with increasing the annealing temperature. The UV–vis spectrum of the colloidal nanoparticles shows maximum absorbance around the UV region optical properties analysis show that hydrothermal technique is a useful method for the deposition of Tetragonal TeO2 thin films on glass substrates. Direct energy band gap values increase with increasing annealing temperatures about 3.9 eV for the film annealed at 673 K for 8 hours.

REFERENCES

[1] M. Naseri, J. Jalilian, and A. H. Rehak, "Electronic and optical properties of paratellurite TeO2 under pressure: A first-principles calculation," *Optik (Stuttg).*, vol. 139, pp. 9–15, 2017.

[2] M. M. Abo Elsoud, O. E. A. Al-Hagar, E. S. Abdelkhalek, and N. M. Sidney, "Synthesis and investigations on tellurium my nanoparticles," *Biotechnol. Reports*, vol. 18, p. e00247, 2018.

[3] Z. Liu, T. Yamazaki, Y. Shen, T. Kikuta, N. Nakatani, and T. Kawabata, "Room-temperature gas sensing of p-type Te O2 nanowires," *Appl. Phys. Lett.*, vol. 90, no. 17, pp. 2–5, 2007.

[4] Z. H. Lin, Y. W. Lin, K. H. Lee, and H. T. Chang, "Selective growth of gold nanoparticles onto tellurium nanowires via a green chemical route," *J. Mater. Chem.*, vol. 18, no. 22, pp. 2569–2572, 2008.

[5] D. Sreedhar, S. Devireddy, and V. Rao Veeredhi, "Facile synthesis and thermal analysis of antimony telluride nanostructures," *Mater. Today Proc.*, vol. 5, no. 2, pp. 5097–5102, 2018.

[6] F. Arab, M. Mousavi-Kamazani, and M. Salavati-Niasari, "Synthesis, characterization, and optical properties of Te, Te/TeO2 and TeO2 nanostructures: Via a one-pot hydrothermal method," *RSC Adv.*, vol. 6, no. 75, pp. 71472–71480, 2016.

[7] M. A. Kamran *et al.*, "Tunable emission and conductivity enhancement by tellurium doping in CdS nanowires for optoelectronic applications," *Phys. E Low-Dimensional Syst. Nanostructures*, vol. 86, no. February 2016, pp. 81–87, 2017.

[8] R. A. Ismail, A. Abid, and A. A. Taha, "Preparation and Characterization of CeO 2 @ Ag Core / Shell Nanoparticles by Pulsed Laser Ablation in Water," vol. 32, no. 4, pp. 3–4, 2019.

[9] P. K. Gupta, P. P. Sharma, A. Sharma, Z. H. Khan, and P. R. Solanki, "Electrochemical and antimicrobial activity of tellurium oxide nanoparticles," *Mater. Sci. Eng. B Solid-State Mater. Adv. Technol.*, vol. 211, pp. 166–172, 2016.

[10] H. Zhang, D. Yang, X. Ma, and D. Que, "Transformation mechanism of Te particles into Te nanotubes and nanowires during solvothermal process," *J. Cryst. Growth*, vol. 289, no. 2, pp. 568–573, 2006.

[11] M. S. Choi *et al.*, "Exploration of the use of p-TeO 2 -branch/n-SnO two core nanowires nanocomposites for gas sensing," *Appl. Surf. Sci.*, vol. 484, no. April, pp. 1102–1110, 2019.

[12] M. Q. Kareem, "Study Optical Properties of (GA) Polysaccharide / Polyvinyl alcohol thin films," vol. 20, pp. 120–124, 2015.

[13] M. Q. Kareem, S. A. Hassan, and M. M. Ameen, "gap of (GA / PVA) composite films," vol. 20, no. 1, pp. 114–119, 2015.